European Journal of Pharmaceutics and Biopharmaceutics 140 (2019) 100–108

Contents lists available at ScienceDirect

European Journal of Pharmaceutics and Biopharmaceutics

journal homepage: www.elsevier.com/locate/ejpb

Research paper

Polyelectrolyte nanocomplexes based on chitosan derivatives for wound healing application

Viorica Patrulea[a], Lee Ann Laurent-Applegate[b], Vasile Ostafe[c,d], Gerrit Borchard[a], Olivier Jordan[a,*]

[a] School of Pharmaceutical Sciences, University of Geneva, University of Lausanne, 1211 Geneva, Switzerland
[b] University Hospital of Lausanne (CHUV-UNIL), Department of Musculoskeletal Medicine, EPCR/02/ch Croisettes 22, 1066 Epalinges, Switzerland
[c] West University of Timisoara, Department of Chemistry, Timisoara 300115, Romania
[d] West University of Timisoara, Advanced Environmental Research Laboratories, Timisoara 300086, Romania

ARTICLE INFO

Keywords:
Chitosan derivative
RGDC
Hydrogel
Polyelectrolyte
Wound healing

ABSTRACT

Wound healing, when compromised, may be guided by biological cues such as Arg-Gly-Asp (RGD), a peptide known to induce cell adhesion and migration, eventually combined with adapted nanocarriers. Three different formulations were prepared and investigated *in vitro* for topical application. All formulations were based on carboxylated and trimethylated chitosan (CMTMC) displaying RGD. The polyelectrolyte nanocomplexes were prepared by mixing two oppositely charged polymers of CMTMC and chondroitin sulfate at different polymer ratios and subsequently characterized by dynamic light scattering and scanning electron microscopy. Hydrogels and foams with a high concentration of RGD-functionalized chitosan (3%) and hyaluronic acid (1.5%) that formed gel-embedded nanocomplexes were developed. *In vitro* assays showed absence of toxicity, ability to promote proliferation over 7 days and promotion of migration of human dermal fibroblasts treated with any of our formulations. These formulations were shown to be suitable for easy topical application and have the potential to accelerate wound healing.

1. Introduction

Dermal wound healing is a complex process, which includes four overlapping steps, namely: inflammation, migration, proliferation and maturation phase [1,2]. In most cases, tissue repair can occur spontaneously, depending on the size and depth of the wound. Failure to heal cutaneous chronic wounds is a major healthcare problem, implying significant annual costs of more than $20 billion in the United States alone and is associated with psychological and physical burden of the patient [3]. Current treatments and management strategies are still inadequate, poorly effective and are often mainly supportive.

The addition of biological cues or bioactive matrices has been widely used to confer functionality improving cell-biomaterial interaction, and more specifically to promote wound healing [4]. In view of this, biopolymers can serve as support for skin reconstruction and therefore reduce or prevent scar formation. In particular, derivatized chitosan matrices have drawn much attention to application in wound care [5–7]. The reactive groups in chitosan (amino group at C2 and hydroxyl groups at C3 and C6) can be chemically modified to provide specific biological functions towards an improvement of tissue regeneration [8,9]. Specifically, the RGD peptide acts as a biological cue which, once properly displayed by an adequate carrier, should guide the fibroblasts for enhanced adhesion, migration and proliferation [10,11]. RGD has been covalently grafted to chitosan derivative for various biomedical applications, enhancing cell adhesion and growth [12,13]. Nanosized particles may be used to efficiently carry and better display the bioactive peptide to the cells, resulting in an increased and prolonged effect [14]. They can be evenly distributed through the wound exudate upon simple addition to a patient's bandage. Moreover, nanocomplexes are both easy to fabricate and to apply *in situ*. In the context of an open, exuding wound, where peptide-grafted polymer substrates are difficult to apply, nanocarriers may be a unique way to display a high density of bioactive peptide to the cells. To this aim, chemically modified chitosan, acting as a cationic water-soluble

Abbreviations: CMTMC, O-carboxymethyl-N,N,N-trimethyl chitosan; DAH, 1,6-diaminohexane; DAH-CMTMC, 1,6-diaminohexane-O-carboxymethyl-N,N,N-trimethyl chitosan; RGDC-DAH-CMTMC, Arg-Gly-Asp-Cys-1,6-diaminohexane-O-carboxymethyl-N,N,N-trimethyl chitosan; NP, nanoparticle; CS, chondroïtin sulfate; HA, hyaluronic acid; HDF, human dermal fibroblast

* Corresponding author.
E-mail address: Olivier.Jordan@unige.ch (O. Jordan).

https://doi.org/10.1016/j.ejpb.2019.05.009
Received 26 October 2018; Received in revised form 9 May 2019; Accepted 10 May 2019
Available online 11 May 2019
0939-6411/

polyelectrolyte can be used. This property helps to trigger the self-assembly of nanosized particles through ionic interactions. As a cationic polyelectrolyte, we used Arg-Gly-Asp-Cys (RGDC) peptide functionalized chitosan derivative (RGDC-DAH-CMTMC) and O-carboxymethyl-N,N,N-trimethylated chitosan (CMTMC) alone as a reference [13]. The 1,6-diaminohexane (DAH) is a 6-carbon spacer arm used to facilitate RGD interaction with cells.

Moreover, as the anionic polyelectrolyte, chondroitin sulfate (CS) can be used, which additionally acts as a growth factor carrier. It reduces inflammatory reactions at the injury sites by interacting with adhesion proteins, cells and extracellular matrix, thus accelerating wound healing [15]. Another polyanionic biopolymer is hyaluronic acid (HA), the main component of the extracellular matrix which is widely used in scaffolding as it helps cells to proliferate and migrate during wound healing [16].

In the case of topical application, formulation is a key issue, which we addressed in our study. In order to improve the delivery of the peptidic moiety, different strategies have been considered: a sprayable suspension of nanoparticles (NPs), a gel and a foam, which would hydrate upon exudate absorption. Hydrogel and foam dressings are preferred for their ability to keep the wound moist to favor healing, to ensure solubilisation of growth factors or antimicrobial agents, and support fibroblast growth [17]. The low adhesion of hydrogels to the wound surface, absorption of exudate and ability to exchange oxygen may also favor healing.

Herein, three different formulations based on the new polymer RGDC-DAH-CMTC were prepared: (*i*) NP suspensions to be applied or sprayed onto the wounds, (*ii*) hydrogels and (*iii*) foam-like patches to serve as wound dressings. CS was used as a carrier for growth factors (in small quantities) for preparing NPs or hyaluronic acid (HA) as a dressing for preparation of the hydrogels or foams. NPs, hydrogels and foams were characterized in terms of their physico-chemical properties, their stability and were evaluated with regard to their toxicity and ability to promote the migration of human dermal fibroblasts.

2. Materials and methods

2.1. RGDC-DAH-CMTMC polymer synthesis

Chitosan derivatives were synthesized as previously reported [13]. Briefly, CMTMC and RGDC-diaminohexane-O-carboxymethyl-N,N,N-trimethyl chitosan (RGDC-DAH-CMTMC) were both synthesized in two steps. First, chitosan (19% degree of acetylation, ChitoClear Cg10, 7–15 mPa·s; Primex, Siglufjordur, Iceland) was trimethylated (at nitrogen at C2 position) to confer positive charges, then carboxymethylated (at hydroxyl groups at C3 and C6) with mono-chloroacetic acid leading to the CMTMC polymer according to previously published protocols (Fig. S1) [18]. A 1,6-diaminohexane (DAH) spacer arm was subsequently added to the carboxyl groups of CMTMC in order to improve RGDC peptide (Bachem, Bubendorf, Switzerland) presentation to the cells and RGDC was grafted to DAH-CMTMC (Fig. S2) [13].

The degree of substitution after each step of the synthesis was checked by ^{1}H NMR (Varian, Gemini 300 MHz, Agilent Technologies, Santa Clara, USA). The peptide grafting was checked by Amino Acid Analysis (AAA; Institut de Biologie Structurale, Grenoble, France). Shortly, for AAA, the final products were hydrolyzed for 45 min at 150 °C in the presence of HCl 6 N/TFA and separated by an ion exchange column. The absorbance was recorded at 570 and 440 nm after post-column derivatization by ninhydrin and the quantity of each amino acid was determined as previously described [13].

2.2. Formation of nanoparticles (NPs) between CMTMC or RGDC-DAH-CMTMC and chondroitin sulfate (CS)

For formation of NP complexes, polymer solutions were dispersed in Milli-Q water at the following concentrations: CMTMC (0.5%); RGDC-DAH-CMTMC (0.5%) and CS (0.1–0.5%) (chondroitin 4- and 6-sulfate at a 40:60 ratio; Sigma–Aldrich GmbH, Buchs, Switzerland). Their ionic interaction and stability depends on the ionization degree of each polyelectrolyte, their mixing ratio, concentration, as well as ionic strength and *p*H of the solution [19]. The *p*H of these solutions was adjusted to 5.7 with 0.1 M HCl. All solutions were filtered through 0.22 µm filters (GE Healthcare Europe GmbH) before their use. Complexation of these dispersed solutions was realized by a "one-shot" method varying the n^{+}/n^{-} ratio [20,21], adding positively charged polyelectrolyte to an oppositely charged polymer, but keeping the same volumetric ratios (1:1). Positive charge from quaternary ammonium was considered (+1) and negative charges from chondroitin sulfate were considered as (−1). Successively, the dispersions were vortexed for 10 sec and separated from the mixture by centrifugation at 20817 × *g* for 10 min at 10 °C. Before re-suspending the NPs in Milli-Q water or trehalose 1%, the supernatant was removed. The NPs were frozen in liquid nitrogen followed by lyophilization at −80 °C and 0.001 mbar using a Christ Alpha 2–4 LD plus freeze-drier (Kuehner AG, Birsfelden, Switzerland). The lyophilizate was re-suspended in pure Milli-Q water before analysis. All the concentrations are given as w/V.

2.3. Hydrogel preparation

Lyophilized CMTMC and hyaluronic acid (HA) of GMP grade of Streptococcus origin (HTL, La Boitardière, France, molecular weight of 1.3–2.2 MDa) were separately dissolved in 0.9% or 1.2% NaCl to reach a concentration range of 1–2% for HA and 2–3% for CMTMC, respectively. The hydrogel samples were obtained by mixing predetermined concentration of CMTMC with HA at a given ratio. The mixture was stirred overnight at room temperature before analysis in order to prevent phase separation occurring for some of the formulations.

2.4. Foam preparation

All foam dressings were prepared in the same way as hydrogels. Afterwards, solutions were stirred overnight at ambient temperature and cast into stainless steel molds of 1x3 cm. The mixture was frozen at −80 °C and lyophilized for 24 h at −80 °C and 0.001 mbar.

2.5. Characterization of formulations

2.5.1. Nanoparticle (NP) characterization

Hydrodynamic diameter (Z-average size), polydispersity index (PDI) and zeta potential (ζ) of the NPs were analyzed by dynamic light scattering (DLS), using a Malvern ZetaSizer Nano ZS (Malvern Instruments, UK) equipped with a 10 mW He/Ne laser beam (λ = 633 nm) at a scattering angle of 173°. All measurements were performed at a temperature of 22 °C in triplicates, each DLS reading was based on 12 repeats.

For long-term stability evaluation of the NPs in aqueous dispersions, particle size distribution, PDI and zeta potential were determined immediately after preparation, 1 h, 1 day and 1 month after NP formation. Moreover, NPs were stored either in water or in 1% trehalose solution (acting as a cryoprotectant), frozen in liquid nitrogen, and lyophilized afterwards. Lyophilization was carried out for 24 h at −80 °C and 0.001 mbar. Before analysis, NPs were re-suspended in water and characterized immediately or after storage at 4 °C for 1 month.

The morphology of lyophilized NPs was investigated using scanning electron microscopy (SEM; JEOL JSM-7001FA, Tokyo, Japan) at an acceleration voltage of 5 kV. The samples were gold coated with a 10 nm sputter coater.

2.5.2. Hydrogel characterization

Rheological studies were performed with a Rheostress 1 Haake rheometer using a cone-plate geometry with a 35 mm/2° Ti cone (Vreden, Germany) thermostated with a circulating bath and a

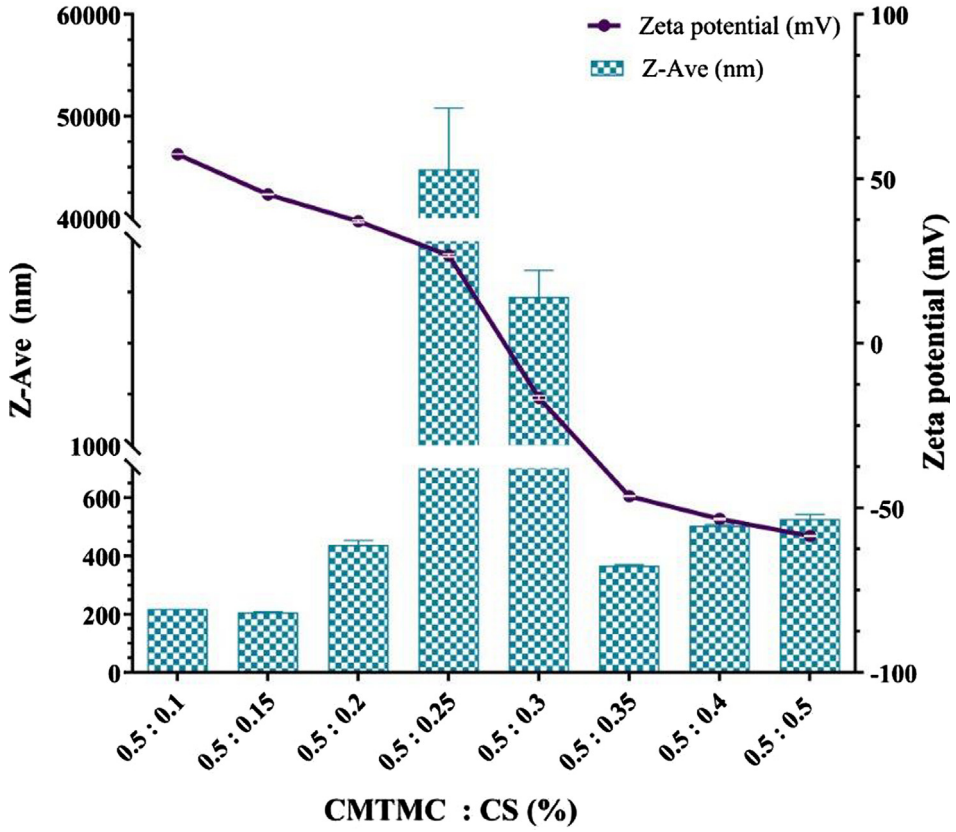

Fig. 1. Average diameter (nm) and zeta potential (mV) of nanoparticles based on CMTMC 0.5% as a function of mixing ratio with CS (%) (n = 3).

programmable controller at 37.0 °C (Haake DC 30) in the 0–3600 s^{-1} shear rate range. In order to prevent water evaporation, a controlled humidity chamber was used.

2.6. WST-1 viability and proliferation assay

For *in vitro* assays, human dermal fibroblasts (HDF, human dermal progenitor cells, 12 weeks male donor, under informed donor consent (Ethics Committee Protocol #62/07, Lausanne, Switzerland)) were used. All cell culture media and additives were purchased from PAN BioTech GmbH (Aidenbach, Germany). The HDF were cultured in Dulbecco's minimal Eagle's medium (DMEM, Gibco, USA) supplemented with 2 mM glutamine (Gibco, USA), 2 mM NaPyr (Gibco, USA) and 10% fetal calf serum (FCS, Hyclone, USA). The cells were split at confluence and the 3^{rd}-7^{th} passages were used for cell seeding.

Viability and proliferation were assessed as cell mitochondrial activity based on the cleavage of tetrazolium salt (4-[3-(4-iodophenyl)-2-(4-nitrophenyl)–2H-5-tetrazolium]-1,3-benzene disulfonate (WST-1), Roche, Switzerland) by mitochondrial dehydrogenases, present in viable cells. HDF were seeded at a density of 2×10^5 cells/mL in a 96-well plate and incubated for 48 h with DMEM to reach confluence. Subsequently, 100 µL of the formulations, either fresh NP suspension or solution of lyophilized foams in DMEM were added.

The viability of cells was evaluated over 2, 4 and 7 days. The formulation solution was changed every three days. The viability and proliferation assays were performed using 100 µL/well of WST-1 solution (1:10 dilution in DMEM) after removing formulation solutions and incubated for 1 h. Absorbance was measured with BioTek Microplate reader (GmbH, Luzern, Switzerland) at 450 nm with a reference at 690 nm. All experiments were carried out in triplicates.

2.7. In vitro scratch migration assay

To investigate the migratory capacity of cells on 2D surfaces, HDF were grown to 100% confluence in a 96-well plate. A fully confluent plate of cells was "wounded" by performing a scratch with a sterile 10 µL micropipette tip. Afterwards, the cell debris was washed with DMEM and cultured with 100 µL of formulation suspension in DMEM with serum for 24 h. The closure of the scratch was followed with a Leica AF6000 LX microscope adapted with CO_2 (5%) and 95% humidity. Every 30 mins cells were photographed under 10X objective lens during 24 h. ImageJ software was used to measure the closure time of the "wounds". All experiments were done in seven replicates.

Foams for the scratch assay were diluted following the protocol described by Rossi et al. [22]. Briefly, 8.7 mg of foam was dissolved in 2 mL of Milli-Q water and then diluted 1:10 with DMEM (with serum) before applying to the cells. Upon hydration, foams led to rapid gel formation having the same composition as the gels. Since same *in vitro* results are expected from foam or gel testing, only foams were evaluated.

2.7.1. Statistical analysis

For both scratch assay and WST-1 test, a two-way Analysis of variance (ANOVA) with Bonferonni's test was used for multiple comparisons using GraphPad Prism 7 (GraphPad Software Inc., USA). A value of $p < 0.05$ was considered statistically significant. Results were expressed as mean ± SEM (standard error of the mean).

3. Results and discussion

The main objective of this study was to develop and evaluate three formulations based on RGDC-functionalized chitosan combined with CS or HA as wound dressings. RGDC is fully soluble at the pH range 4–7.5. Cationic chitosan derivatives, owing to its positive charges from

Table 1
Nanoparticles ratio n^+/n^-, size, zeta potential and polydispersity index (PDI) for varying concentration of CS (n = 3).

CMTMC (%)	CS (%)	Ratio (n^+/n^-)	Size (nm)	Zeta (mV)	PDI
0.5	0.1	2.37	217.7 ± 1.2	57.4 ± 0.05	0.25 ± 0.005
0.5	0.15	1.58	206.4 ± 2.9	45.2 ± 0.1	0.23 ± 0.006
0.5	0.2	1.19	437.0 ± 28.5	37.1 ± 0.7	0.43 ± 0.030
0.5	0.25	0.95	$44 \times 10^3 \pm 10^4$	26.7 ± 0.8	0.76 ± 0.190
0.5	0.3	0.79	$1.5 \times 10^3 \pm 178.1$	−16.5 ± 1.0	0.98 ± 0.04
0.5	0.35	0.68	366.5 ± 4.9	−46.4 ± 0.3	0.36 ± 0.006
0.5	0.4	0.60	503.0 ± 7	−53.3 ± 0.4	0.44 ± 0.010
0.5	0.5	0.48	525.4 ± 28.6	−58.5 ± 0.2	0.49 ± 0.090

trimethyl amino groups, were used as carriers of RGD biological cue to enable nanoparticle formation by ionic gelation as well as gel formulation in view of guiding fibroblasts towards wound healing process.

3.1. Influence of polyelectrolytes ratio on NPs physicochemical properties

^{1}H NMR analysis of CMTMC showed degrees of substitution of 0.36 for N,N,N-trimethylation, and 0.9 for O-carboxymethylation (Supplementary Fig. S3). AAA showed that RGDC was grafted to the chitosan backbone at a density of 15.3 µg per 1 mg of chitosan derivative [13].

NPs were obtained by addition of CS to an excess of chitosan derivatives (CMTMC or RGDC-DAH-CMTMC) in aqueous phase to obtain different surface charges. Fig. 1 shows the Z-average mean diameter of NPs composed of CMTMC: CS and their zeta potential. Having a sufficiently high zeta potential allows the use of NPs as carriers for drugs or proteins through ionic interactions [23]. Table 1 gives more detailed numerical information including polydispersity index (PDI).

For charge ratio n^+/n^- of 0.79 and 0.95, close to 1, larger complexes with broad size distribution were obtained, leading to flocculation. This could be attributed to poor colloidal stability arising from low absolute value of zeta potential (< 30 mV). NPs obtained from CMTMC: CS ratio of 0.5: 0.1 lead to stable, small cationic nanocomplexes and were selected for further *in vitro* investigation.

A similar aggregation effect was observed in the case of RGDC-DAH-CMTMC (Fig. 2). Close to $n^+/n^- = 1$, when 0.2% of CS was added, large aggregates were formed. In contrast, a 0.1% CS concentration formed cationic NPs. Increasing CS concentration to 0.3% led to anionic, stable NPs with a size of 216.9 ± 1.3 nm (PDI = 0.1) and a zeta potential of −40.9 ± 0.2 mV. Therefore, the RGDC-DAH-CMTMC/CS nanocomplexes were obtained in the 200 nm range with either cationic or anionic charges.

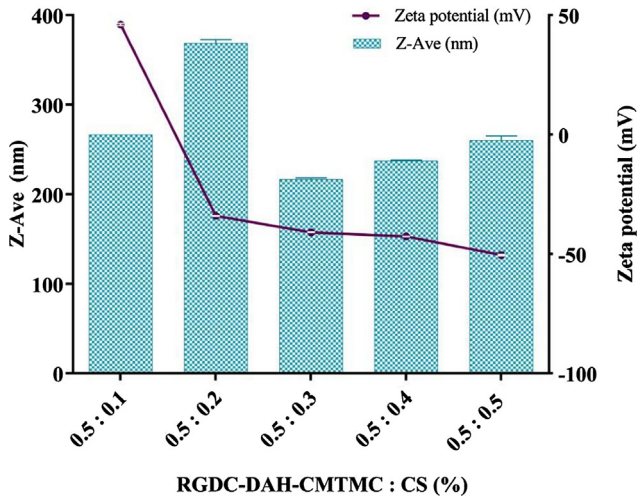

Fig. 2. Sizes and zeta potential of nanoparticles based on RGDC-DAH-CMTMC 0.5% complexation with different CS concentration (n = 3).

SEM images of the lyophilized NPs in water are presented in Fig. 3. These images showed a spherical shape and well-defined NPs based on both CMTMC 0.5% with CS 0.1% (Fig. 3a) and RGDC-DAH-CMTMC 0.5% with CS 0.3% (Fig. 3b). NPs based on ratios 0.5:0.1 CMTMC:CS and 0.5:0.3 RGDC-DAH-CMTMC:CS were selected for further *in vitro* experiments, for their small size (ca. 220 nm) and low PDI, suggesting absence of aggregates.

Furthermore, a critical factor is to maintain both NPs colloidal stability for long-term storage and NPs integrity, by finding the balance between the inter-particle and intermolecular forces, respectively.

Therefore, NPs were characterized for their size, surface charge and PDI under different storage conditions over 1 month (Fig. 4). It was observed that NPs stored in water at 4° C were no longer stable after 1 month, neither immediately after lyophilization/re-suspension in water (size ~4000 nm). However, flocculation after lyophilization in water or after 1 month of storage was observed, attributed to the freezing stress followed by dehydration stress and crystallization of ice [24]. For this very reason, trehalose was chosen as cryoprotectant in order to allow long-term storage and resuspension of the nanoparticles. Therefore, NPs lyophilized and stored in a trehalose 1% solution, maintained the same size before and after lyophilization. Herein, RGDC-bearing NPs (0.5: 0.3) showed a preserved size of approximately 200 nm (PDI ~0.2) and were less negatively charged (−40 mV) when reconstituted from a 1 month-stored lyophilized formulation in trehalose. As most of the guidelines advise to use NPs with a size range between 100 and 250 nm for the NPs to remain in the wounded area [25], we focused on this specific size.

3.2. Rheological behavior of hydrogels formulations

In parallel, hydrogels and foams were formulated, that would have favorable properties for topical application and wound moisturizing. Gels composed of oppositely charged polyelectrolytes generally flocculate, which impedes pharmaceutical use. However, adding specific counterions may allow homogeneous gel formation [26]. Here, we combined CMTMC and HA adding NaCl 0.9 or 1.2%, which led to the formation of polyelectrolyte nanocomplexes embedded in a viscous gel, to be used for topical application. The chitosan amount was maximized in view of an increased RGDC peptide content of the derivatized chitosan and, in turn, with a higher bioactivity. Gels for topical application require a high viscosity to maintain their shape, with some “gel-like” elasticity.

First, viscoelastic analysis in oscillatory rheological mode was performed (Fig. 5). High but relatively similar values for storage modulus G’ and loss modulus G” reflected the dual viscous and elastic nature of the formulations. Crossover frequencies for G’ and G”, which indicate gel-sol transitions, occurred at 0.4 Hz for the HA 2.0%/CMTMC 3% and 2 Hz for the HA 1.5%/CMTMC 3% formulations. This demonstrates that both formulations may be characterized as “gels” at the low frequency at which they will be used and applied on the skin.

Beside their “gel-like” behavior, topical formulations would benefit from shear-thinning rheological behavior for ease of application, as investigated by rotational viscosimetry.

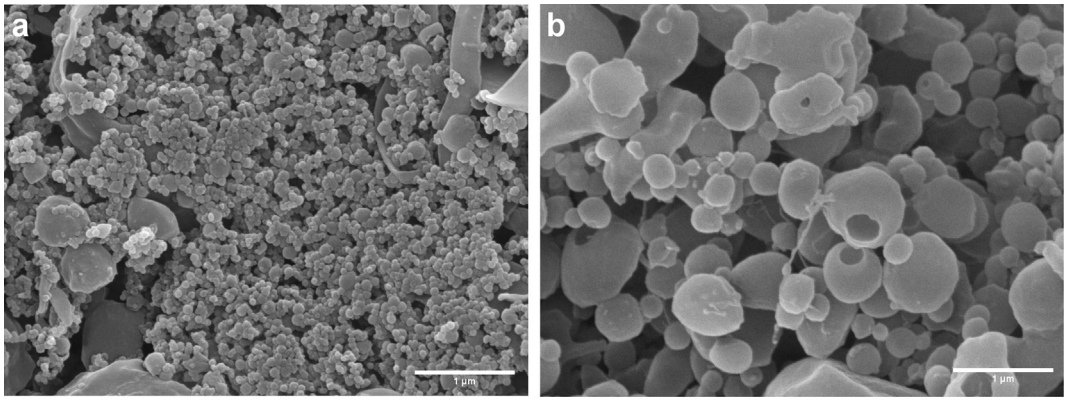

Fig. 3. SEM images of selected (a) CMTMC and (b) RGDC-DAH-CMTMC nanoparticles selected for further *in vitro* experiments. The scale bars represent 1 µm.

Fig. 6 displays gel dynamic viscosity decreasing with shear rate. The curve corresponding to the hydrogel composed of HA 1.0% and CMTMC 3.0% was omitted due to its superposition with the HA 1.0% CMTMC 2.5% curve. A rheofluidifying behavior was observed for all concentrations, fitting to an Ostwald power law model (Eq. (1) and Table 2).

$$\eta = K \bullet \gamma^{n-1} \quad (1)$$

where η is viscosity of the hydrogel, γ represents the shear rate, K the flow consistency index, reflecting the viscosity (or stress) at a shear rate of 1 s^{-1} and n is the flow behavior index indicating the non-Newtonian or Newtonian character [27].

A power-law relationship is observed ($R^2 > 0.98$ for all formulations). A value of $n > 1$ involving a shear-thickening effect was only observed for the low viscosity HA 0.5% CMTMC 3.0% formulation. In contrast, all other formulations had flow behavior index $n < 1$, indicating a shear-thinning or rheofluidifying behavior (Table 2). The viscosity of the CMTMC/HA hydrogels was shown to increase as a function of polymer concentration, still allowing an easy skin application at highest evaluated concentration. Higher gel concentrations might also be considered, however at the cost of a reduced ease of application and ability to conform to an irregularly shaped wound.

Beside the absence of flocculation, another stability requirement is the absence of phase separation or syneresis. Concentrations of 0.5% of HA with 3.0% CMTMC, which led to a clear phase separation in both 0.9% and 1.2% NaCl were thus not retained (Fig. S4). Additionally, high gel viscosity, as obtained with HA 1.5% or 2%, would be preferred for application on wounds, combined with a high content in chitosan derivative (3%) at physiological saline concentration (preferred gels formulations outlined in bold, Table 2).

3.3. Foam-like formulations

Following lyophilization, some foams were brittle and difficult to handle due to their fragility. Decreasing salt concentration from 1.2 to 0.9% resulted in softer, much less brittle formulations. Specifically, high HA concentration (1.5% and 2%) prepared in NaCl 0.9% led to soft foams after lyophilization. These flexible foams were sufficiently tough to be easily handled without breaking. Foam brittleness may be due to lower inter- and intra-molecular hydrogen interactions. As a result, the compactness of the foams is diminished leading to very weak mechanical properties. Although flexible, higher HA concentration (2%) resulted in macroscopically inhomogeneous foams with many bubbles. Only formulations based on CMTMC 3% (or RGDC-DAH-CMTMC 3%) and HA 1.5% were flexible, not fragile and homogeneous, thus **selected for further experiments**.

Both lyophilized foams, with and without RGDC peptide, showed a porous and interconnected structure. SEM of CMTMC/HA foams (Fig. 7a) indicated highly porous networks produced by lyophilization, with pore sizes ranging from 100 to 200 µm. RGDC-DAH-CMTMC/HA foams (Fig. 7b) showed tight microstructures with a smaller pore diameter in the 20 to 100 µm range, which may indicate stronger ionic

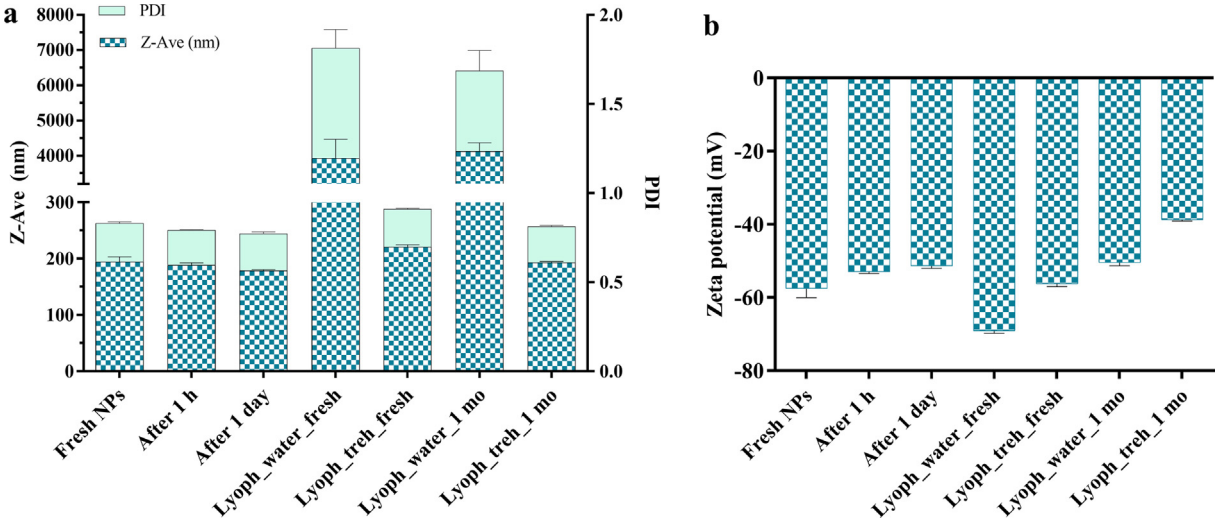

Fig. 4. Stability of nanoparticles formed from RGDC-DAH-CMTMC by complexation with CS. The size, PDI (a) and zeta potential (b) were evaluated over 1 month under different conditions. Lyophilized formulations were eventually added with trehalose as cryo-protectant ("Lyoph" stands for lyophilisation, "treh" for trehalose and "mo" for month).

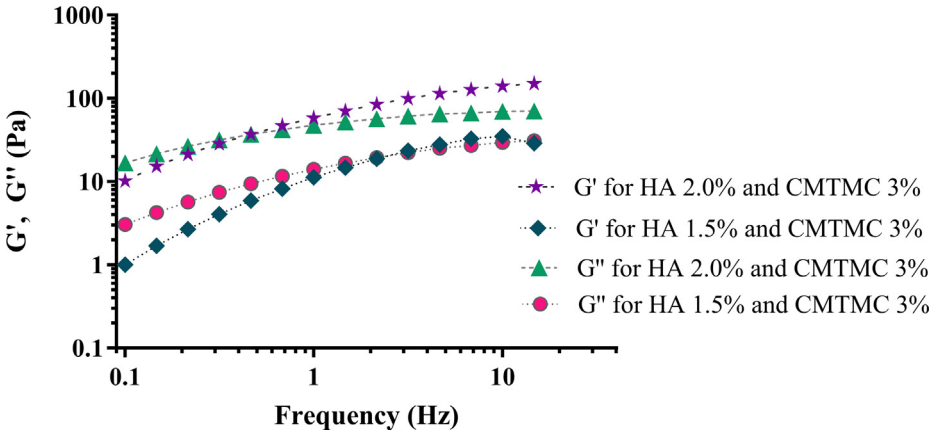

Fig. 5. Viscoelastic values G′and G″ as a function of frequency for mixtures HA and CMTMC.

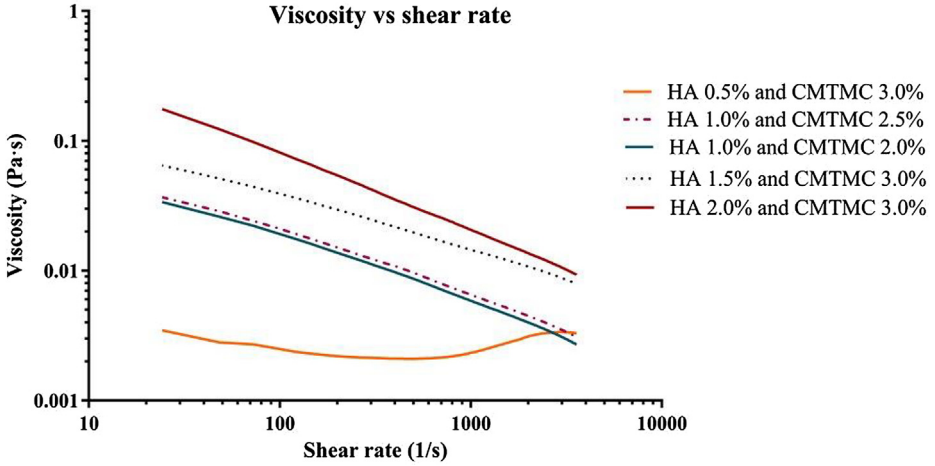

Fig. 6. Viscosity profiles of CMTMC/HA formulations in NaCl 0.9% as a function of shear rate.

Table 2
Rheological Ostwald-de Waele coefficients: n, flow behavior index and K, flow consistency index.

NaCl concentration (%)	Polymer		Coefficients	
	HA (%)	*CMTMC (%)*	*n*	*K*
0.9	0.5	3.0	1.13	0.001
	1.0	2.0	0.46	0.24
	1.0	2.5	0.47	0.25
	1.0	3.0	0.81	0.04
	1.5	**3.0**	**0.56**	**0.30**
	2.0	**3.0**	**0.40**	**1.29**
1.2	0.5	3.0	0.85	0.005
	1.0	2.0	0.60	0.28
	1.0	2.5	0.44	0.96
	1.0	3.0	0.48	0.19
	1.5	3.0	0.45	1.18
	2.0	3.0	0.33	5.39

interactions in the parent hydrogel [28].

3.4. Formulations safety: In vitro testing on fibroblasts

The following selected formulations were evaluated for their toxicity using WST-1 assay: NPs based on CMTMC: CS (0.5%: 0.1%) and RGDC-DAH-CMTMC: CS (0.5%: 0.3%); hydrogels based on lyophilized foams of CMTMC or RGDC-DAH-CMTMC and HA (3.0% in 1.5%). Freshly prepared NPs (with and without RGDC) were diluted in 1 mL DMEM (containing 10% FCS) while foams were prepared corresponding to Rossi et al. protocol for dressings [22] and exposed to HDF at final polymer concentrations of 0.5% (w/w).

After 2 and 4 days of exposure to NPs or hydrated foams formulations, no notable decrease of mitochondrial activity, thus presumably of cell viability was observed (> 85%). After 7 days, the high mitochondrial activity for all formulations (> 85%) compared to the positive cell controls (tissue culture plate (TCP) treated) suggested an enhanced proliferation of HDFs in the presence of NPs or hydrated foams of CMTMC or RGDC-DAH-CMTMC (Fig. 8). This latter time point mimics the “formulation-tissue” contact time, which is of interest for topical wound healing bandage application. Cells treated with foams based on RGDC-functionalized chitosan induced more proliferation than CMTMC formulations ($p < 0.05$; Fig. 8). This observation is in agreement with previous reports indicating that RGD-functionalized biomaterials may not only improve adhesion but also proliferation of fibroblasts [29]. Other studies, using similar MTT assay on fibroblasts, reported no toxicity of chitosan [30] or carboxymethyl chitosan [31]. Still, this study is the first report showing that nanoformulations based on RGDC-derivatized chitosan can have a significant effect on proliferation.

3.5. Effect of RGD-tailored formulations on fibroblast migration

Based on the tolerability of these formulations and the ability of the polymer to promote fibroblast proliferation, the nanocomplexes and foam formulations bearing RGDC were used to assess their activity towards fibroblast migration, by measuring the closure of a “wound” in a scratch assay (Fig. 9).

No significant differences ($p \geq 0.05$) were observed at 12 h and 24 h

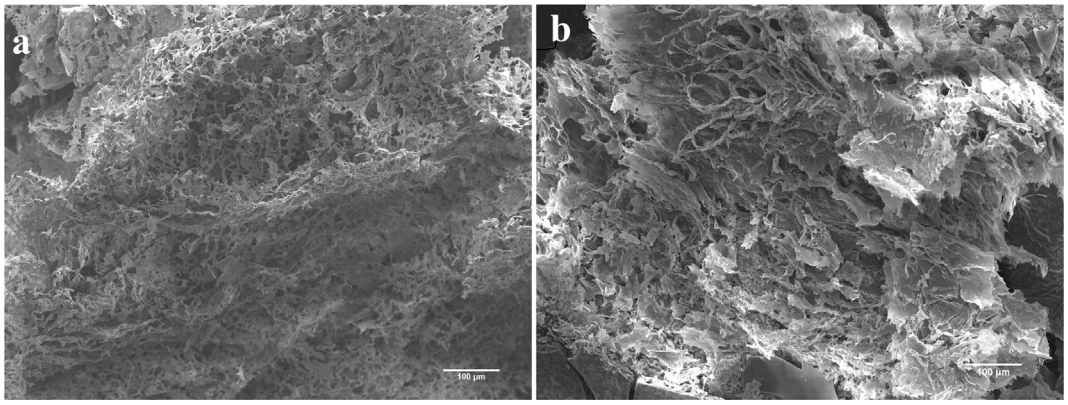

Fig. 7. Scanning electron micrographs showing network structure of CMTMC/HA lyophilized foams: (a) CMTMC 3% and HA 1.5% in NaCl 0.9% and (b) RGDC-DAH-CMTMC 3% and HA 1.5% in NaCl 0.9%, both selected for further experiments . The scale bars represent 100 µm.

when comparing migration of fibroblasts treated with either the foam or NPs with TCP treated cells (control). Microscopy analysis showed that cells in the presence of foams have a more elongated phenotype with cellular orientation and migration in one direction when compared with cells in the presence of NPs or TCP. Migration assay were also performed with CMTMC, but did not lead to significant wound closure, attributed to a partial aggregation of the polymer in presence of cell's physiological media.

Fibroblast migration, along with proliferation, is the most important phenomenon during the second phase of wound healing [32]. All the intrinsic or extrinsic factors that alter these steps will negatively influence the normal process of wound healing. We have shown that our formulations do not alter the migration of fibroblasts and that cells incubated for 24 h with these compounds are able to migrate and fill the scratch in an *in vitro* wound healing assay at the same rate as the migration-conducive treated TCP substrate (Fig. 9).

In order to promote cell adhesion and spreading, biomaterials can be modified before getting in contact with the cells by introducing cell-binding motif to the polymeric matrix backbone [33]. Studies bear out that cells from patients cannot integrate efficiently into various formulations of biomaterials including hydrogels and foams, and many of these have proven to be toxic to the patient cells [34]. However, it was shown that commercially available matrix such as TissuFleece® resulted in randomly distributed cell aggregates within the matrix and it may induce extensive scarring [34]. As well, AlloDerm®, was shown to limit cell penetration into the matrix due to its dense structure resulting in HDF proliferation in layers only at matrix's periphery. Therefore, AlloDerm may be used more as a cell-free matrix [34,35].

The main objective of this study was to develop and evaluate three formulations based on RGDC-functionalized chitosan combined with CS or HA as wound dressings. Cationic chitosan derivatives, bearing positive charges from trimethyl amino groups, were formulated as carriers of biological cues that guide fibroblasts towards wound healing process.

These observations suggest that our formulations would have a favorable effect on the wound healing process. Still, further investigations and animal studies are needed to confirm this effect *in vivo*.

4. Conclusions

Despite the large number of biomaterials reported for topical wound healing, limitations in terms of poor mechanical properties, lack of migration promotion or risk of immunological reactions still remain. The proposed nanocomplexes based on chitosan derivatives were shown to preserve RGD peptide bioactivity, allowing complete gap closure in an *in vitro* wound scratch assay model. These results were attributed to the presence of the RGD adhesive peptide. Moreover,

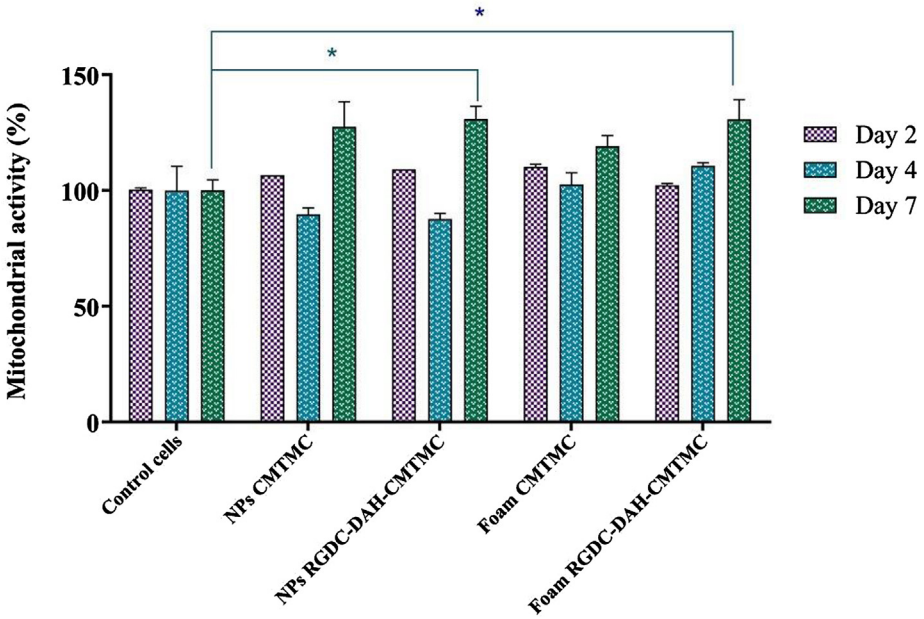

Fig. 8. WST-1 assay on HDFs for the selected formulations (n = 3) (*p < 0.05).

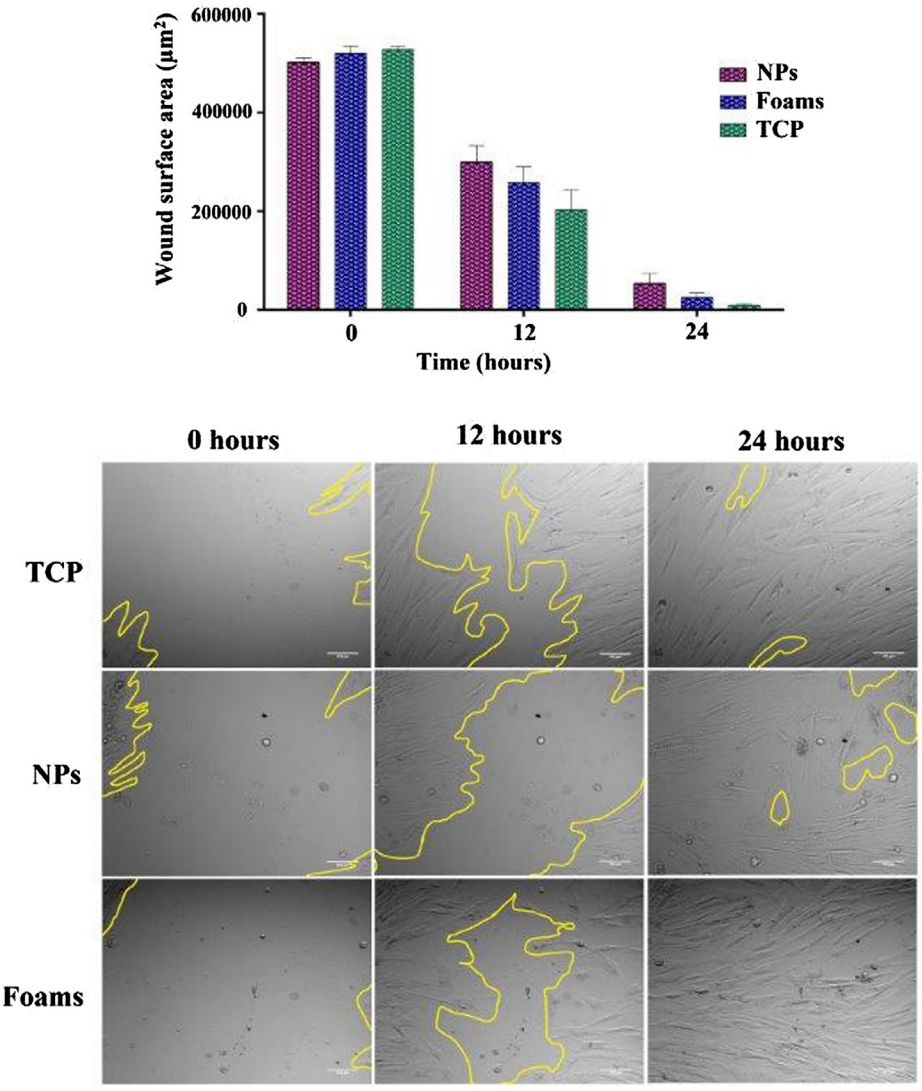

Fig. 9. Wound surface area graph and bright field images for wound closure at time at time 0, 12 and 24 h using scratch assay (n = 7). No statistical difference at 24 h between TCP treated cells and formulations ($p \geq 0.05$).

RGDC-DAH-CMTMC nanoformulations demonstrated no toxicity towards HDF and promoting their adhesion and proliferation by 30% over 1 week.

Such nanostructured formulations based on adhesion-promoting peptides may stimulate wound healing, and deserve further *in vitro* and *in vivo* evaluation. Moreover, derivatization of DAH-CMTMC is a technological platform allowing controlled addition of a variety of peptides or growth factors towards promotion or acceleration of tissue healing and regeneration. Reported results may contribute to the design of chitosan-based formulations such as viscous gels, foams and nanoparticles for topical application.

Acknowledgements:

This work was supported by Sciex-NMS [grant 12.191]. We thank Primex (Iceland) for their kind donation of chitosan. We are grateful to Mr. Tayeb Jbilou (University of Geneva, Geneva, Switzerland) for the assistance for scanning electron microscopy and both Dr. Nathalie Hirt-Burri and Dr. Paris Jafari (Centre Hospitalier Universitaire Vaudois, Lausanne, Switzerland) for their technical advice on cellular assays.

Appendix A. Supplementary material

Supplementary data to this article can be found online at https://doi.org/10.1016/j.ejpb.2019.05.009.

References

[1] D. Archana, J. Dutta, P.K. Dutta, Evaluation of chitosan nano dressing for wound healing: Characterization, in vitro and in vivo studies, Int. J. Biol. Macromol. 57 (2013) 193–203, https://doi.org/10.1016/j.ijbiomac.2013.03.002.
[2] G. Grieb, G. Steffens, N. Pallua, J. Bernhagen, R. Bucala, Circulating fibrocytes - biology and mechanisms in wound healing and scar formation, Int. Rev. Cell Mol. Biol. 291 (2011) 1–19.
[3] K. Järbrink, G. Ni, H. Sönnergren, A. Schmidtchen, C. Pang, R. Bajpai, J. Car, The humanistic and economic burden of chronic wounds: a protocol for a systematic review, Syst. Rev. 6 (2017) 15, https://doi.org/10.1186/s13643-016-0400-8.
[4] U. Hersel, C. Dahmen, H. Kessler, RGD modified polymers: biomaterials for stimulated cell adhesion and beyond, Biomaterials 24 (2003) 4385–4415, https://doi.org/10.1016/S0142-9612(03)00343-0.
[5] V. Patrulea, V. Ostafe, G. Borchard, O. Jordan, Chitosan as a starting material for wound healing applications, Eur. J. Pharm. Biopharm. 97, B (2015) 417–426, https://doi.org/10.1016/j.ejpb.2015.08.004.
[6] P.T. Sudheesh Kumar, N.M. Raj, G. Praveen, K.P. Chennazhi, S.V. Nair, R. Jayakumar, In vitro and in vivo evaluation of microporous chitosan hydrogel/nanofibrin composite bandage for skin tissue regeneration, Tissue Eng. Part A 19 (2013) 380–392, https://doi.org/10.1089/ten.TEA.2012.0376.
[7] H. Ueno, T. Mori, T. Fujinaga, Topical formulations and wound healing applications of chitosan, Adv. Drug Deliv. Rev. 52 (2001) 105–115, https://doi.org/10.1016/

S0169-409X(01)00189-2.
[8] N. Boucard, C. Viton, D. Agay, E. Mari, T. Roger, Y. Chancerelle, A. Domard, The use of physical hydrogels of chitosan for skin regeneration following third-degree burns, Biomaterials 28 (2007) 3478–3488, https://doi.org/10.1016/j.biomaterials.2007.04.021.
[9] I.M. Van Der Lubben, J.C. Verhoef, G. Borchard, H.E. Junginger, Chitosan for mucosal vaccination, Adv. Drug. Deliv. Rev. 52 (2001) 139–144, https://doi.org/10.1016/S0169-409X(01)00197-1.
[10] E. Ruoslahti, RGD and other recognition sequences for integrins, Annu. Rev. Cell Dev. Biol. 12 (1996) 697–715, https://doi.org/10.1146/annurev.cellbio.12.1.697.
[11] G. Tarone, E. Hirsch, M. Brancaccio, M. De Acetis, L. Barberis, F. Balzac, S.F. Retta, C. Botta, F. Altruda, L. Silengo, Integrin function and regulation in development, Int. J. Dev. Biol. 44 (2000) 725–731.
[12] W.-B. Tsai, Y.-R. Chen, W.-T. Li, J.-Y. Lai, H.-L. Liu, RGD-conjugated UV-crosslinked chitosan scaffolds inoculated with mesenchymal stem cells for bone tissue engineering, Carbohydr. Polym. 89 (2012) 379–387, https://doi.org/10.1016/j.carbpol.2012.03.017.
[13] V. Patrulea, N. Hirt-Burri, A. Jeannerat, L.A. Applegate, V. Ostafe, O. Jordan, G. Borchard, Peptide-decorated chitosan derivatives enhance fibroblast adhesion and proliferation in wound healing, Carbohydr. Polym. 142 (2016) 114–123, https://doi.org/10.1016/j.carbpol.2016.01.045.
[14] S. Bhatia, Nanoparticles types, classification, characterization, fabrication methods and drug delivery applications, Natural Polymer Drug Delivery Systems: Nanoparticles, Plants, and Algae, Springer International Publishing, Cham, 2016, pp. 33–93.
[15] J.-J. Young, C.-C. Chen, Y.-C. Chen, K.-M. Cheng, H.-J. Yen, Y.-C. Huang, T.-N. Tsai, Positively and negatively surface-charged chondroitin sulfate-trimethylchitosan nanoparticles as protein carriers, Carbohydr. Polym. 137 (2016) 532–540, https://doi.org/10.1016/j.carbpol.2015.10.095.
[16] S.A. De Oliveira, B.C. Da Silva, I.C. Riegel-Vidotti, A. Urbano, P.C. De Sousa Faria-Tischer, C.A. Tischer, Production and characterization of bacterial cellulose membranes with hyaluronic acid from chicken comb, Int. J. Biol. Macromol. 97 (2017) 642–653, https://doi.org/10.1016/j.ijbiomac.2017.01.077.
[17] R. Jayakumar, M. Prabaharan, P.T. Sudheesh Kumar, S.V. Nair, H. Tamura, Biomaterials based on chitin and chitosan in wound dressing applications, Biotechnol. Adv. 29 (3) (2011) 322–337, https://doi.org/10.1016/j.biotechadv.2011.01.005.
[18] V. Patrulea, L.A. Applegate, V. Ostafe, O. Jordan, G. Borchard, Optimized synthesis of O-carboxymethyl-N, N N-trimethyl chitosan, Carbohydr. Polym. 122 (2015) 46–52, https://doi.org/10.1016/j.carbpol.2014.12.014.
[19] J.H. Hamman, Chitosan based polyelectrolyte complexes as potential carrier materials in drug delivery systems, Mar. Drugs 8 (2010) 1305–1322, https://doi.org/10.3390/md8041305.
[20] A. Hansson, T. Di Francesco, F. Falson, P. Rousselle, O. Jordan, G. Borchard, Preparation and evaluation of nanoparticles for directed tissue engineering, Int. J. Pharm. 439 (2012) 73–80, https://doi.org/10.1016/j.ijpharm.2012.09.053.
[21] C. Schatz, A. Domard, C. Viton, C. Pichot, T. Delair, Versatile and efficient formation of colloids of biopolymer-based polyelectrolyte complexes, Biomacromolecules 5 (2004) 1882–1892, https://doi.org/10.1021/bm049786+.
[22] S. Rossi, A. Faccendini, M.C. Bonferoni, F. Ferrari, G. Sandri, C. Del Fante, C. Perotti, C.M. Caramella, “Sponge-like” dressings based on biopolymers for the delivery of platelet lysate to skin chronic wounds, Int. J. Pharm. 440 (2013) 207–215, https://doi.org/10.1016/j.ijpharm.2012.07.056.
[23] Q. Gan, T. Wang, C. Cochrane, P. Mccarron, Modulation of surface charge, particle size and morphological properties of chitosan–TPP nanoparticles intended for gene delivery, Colloids Surf., B 44 (2005) 65–73, https://doi.org/10.1016/j.colsurfb.2005.06.001.
[24] W. Abdelwahed, G. Degobert, S. Stainmesse, H. Fessi, Freeze-drying of nanoparticles: formulation, process and storage considerations, Adv. Drug Deliv. Rev. 58 (2006) 1688–1713, https://doi.org/10.1016/j.addr.2006.09.017.
[25] M. Ashtikar, M.G. Wacker, Nanopharmaceuticals for wound healing - Lost in translation? Adv. Drug Deliv. Rev. 129 (2018) 194–218, https://doi.org/10.1016/j.addr.2018.03.005.
[26] S. Kaderli, C. Boulocher, E. Pillet, D. Watrelot-Virieux, A.L. Rougemont, T. Roger, E. Viguier, R. Gurny, L. Scapozza, O. Jordan, A novel biocompatible hyaluronic acid-chitosan hybrid hydrogel for osteoarthrosis therapy, Int. J. Pharm. 483 (2015) 158–168, https://doi.org/10.1016/j.ijpharm.2015.01.052.
[27] G.A. Hurst, M. Bella, C.G. Salzmann, The Rheological Properties of Poly(vinyl alcohol) Gels from Rotational Viscometry, J. Chem. Educ. 92 (2015) 940–945, https://doi.org/10.1021/ed500415r.
[28] F. Ahmadi, Z. Oveisi, S.M. Samani, Z. Amoozgar, Chitosan based hydrogels: characteristics and pharmaceutical applications, Res. Pharm. Sci. 10 (1) (2015) 1–16.
[29] Y.D. Park, N. Tirelli, J.A. Hubbell, Photopolymerized hyaluronic acid-based hydrogels and interpenetrating networks, Biomaterials 24 (2003) 893–900, https://doi.org/10.1016/S0142-9612(02)00420-9.
[30] G.I. Howling, P.W. Dettmar, P.A. Goddard, F.C. Hampson, M. Dornish, E.J. Wood, The effect of chitin and chitosan on the proliferation of human skin fibroblasts and keratinocytes in vitro, Biomaterials 22 (2001) 2959–2966, https://doi.org/10.1016/S0142-9612(01)00042-4.
[31] X.-G. Chen, Z. Wang, W.-S. Liu, H.-J. Park, The effect of carboxymethyl-chitosan on proliferation and collagen secretion of normal and keloid skin fibroblasts, Biomaterials 23 (2002) 4609–4614, https://doi.org/10.1016/S0142-9612(02)00207-7.
[32] M.N.M. Walter, K.T. Wright, H.R. Fuller, S. Macneil, W.E.B. Johnson, Mesenchymal stem cell-conditioned medium accelerates skin wound healing: An in vitro study of fibroblast and keratinocyte scratch assays, Exp. Cell Res. 316 (2010) 1271–1281, https://doi.org/10.1016/j.yexcr.2010.02.026.
[33] K. Ghosh, X.-D. Ren, X.Z. Shu, G.D. Prestwich, R.F. Clark, Fibronectin functional domains coupled to hyaluronan stimulate adult human dermal fibroblast responses critical for wound healing, Tissue Eng. 12 (2006) 601–613, https://doi.org/10.1089/ten.2006.12.601.
[34] K.W. Ng, H.L. Khor, D.W. Hutmacher, In vitro characterization of natural and synthetic dermal matrices cultured with human dermal fibroblasts, Biomaterials 25 (2004) 2807–2818, https://doi.org/10.1016/j.biomaterials.2003.09.058.
[35] A.P. Sclafani, T. Romo 3rd, A.A. Jacono, S. Mccormick, R. Cocker, A. Parker, Evaluation of acellular dermal graft in sheet (AlloDerm) and injectable (micronized AlloDerm) forms for soft tissue augmentation. Clinical observations and histological analysis, Arch. Facial Plast. Surg. 2 (2000) 130–136.